Numerical on-the-fly implementation of the action of the kinetic energy operator on a vibrational wave function: application to methanol

André Nauts, David Lauvergnat

Numerical on-the-fly implementation of the action of the kinetic energy operator on a vibrational wave function: application to methanol

André Nauts[a,b] and David Lauvergnat[b*]

a) Institute of Condensed Matter and Nanosciences (NAPS), Université Catholique de Louvain, 2 Chemin du Cyclotron, bte L7.01.07, B-1348 Louvain-la-Neuve, Belgium.

b) Laboratoire de Chimie Physique, CNRS, Univ. Paris-Sud, Université Paris-Saclay, 91405, Orsay, France.

* Corresponding author: David.Lauvergnat@lcp.u-psud.fr

Keywords: Torsional level, Methanol, Kinetic energy operator, On-the-fly

Abstract

In quantum dynamics, physically well-adapted curvilinear coordinates are coordinates that lead to a Hamiltonian operator as separable as possible, in order to simplify the resolution of the corresponding time-independent or time-dependent Schrödinger equations. Various equivalent curvilinear expressions of the kinetic energy operator (KEO) are well known. They can be used in either an analytical or a numerical approach. The latter has the feature of allowing to straightforwardly compute the KEO in terms of sophisticated (yet easy to define) physically well-adapted curvilinear coordinates. Nevertheless, the number of terms to be computed on a full grid, scales as $n^2/2$ (n being the number of degrees of freedom), so that, for systems with $n>10$, the memory storage of the KEO's becomes extremely demanding and therefore often unrealistic. We show here that it is possible, starting from the basic quantum expression of the KEO as a curvilinear Laplacian operator, to reduce the memory storage bottleneck by numerically computing the KEO *on-the-fly* i.e. each time it is required without computing the extrapotential term. This new approach opens the way to rigorous quantum studies of systems with many degrees of freedom.

The comparison of torsional levels of methanol obtained by the present *on-the-fly* method with our previous results shows excellent agreement.

I Introduction

In molecular physics it is often essential for solving problems efficiently to use curvilinear coordinates (such as bond lengths, bond angles, torsional angles…) physically well adapted to the molecular systems and the processes under study. Indeed, an optimal set of curvilinear coordinates has to lead to a Hamiltonian operator that is as separable as possible, *i.e.* that reduces as much as possible the coupling terms between the coordinates, in order to simplify the resolution of the corresponding time-independent or time-dependent Schrödinger equations.

The quantum kinetic energy operator, KEO, has various well-known equivalent expressions in terms of curvilinear coordinates [1][2][3][4][5]. These expressions lead to two main approaches: (i) an analytical one, adapted to particular sets of coordinates, such as Jacobi or polyspherical coordinates [6][7][8]. (ii) a numerical one, [9][10][11][12][13][14] particularly well-suited when sophisticated physically well-adapted coordinates are needed. For instance, with TNUM, [12][15][16] it is possible to successively perform several coordinate transformations (symmetrized coordinates, flexible coordinates, curvilinear normal modes, coordinates associated with a reaction-path Hamiltonian [17][18][16]…).

Let the configuration of an *N*-atom molecular system be described by means of *n* curvilinear coordinates $\boldsymbol{Q} = [Q^1, \cdots Q^i, \cdots Q^n]$. The standard quantum expression of the KEO in terms of *n* curvilinear coordinates is given by the following Laplacian operator [1][2][3][4][5]:

$$\hat{T}_J(\boldsymbol{Q}, \partial_{\boldsymbol{Q}}) = -\frac{\hbar^2}{2} \sum_{i=1}^{n} \frac{1}{J(\boldsymbol{Q})} \frac{\partial .}{\partial Q^i} J(\boldsymbol{Q}) \sum_{j=1}^{n} G^{ij}(\boldsymbol{Q}) \frac{\partial .}{\partial Q^j} \qquad \text{Eq. 1a}$$

and $d\tau_J = J(\boldsymbol{Q}) dQ^1 \cdots dQ^n$ Eq.1b

where the $G^{ij}(\boldsymbol{Q})$ (*i,j*=1...*n*) are the contravariant components of the metric tensor, $\boldsymbol{G}(\boldsymbol{Q})$, and where $J(\boldsymbol{Q}) = \det(\boldsymbol{G}(\boldsymbol{Q}))^{-1/2}$. $J(\boldsymbol{Q})$ is also used to define the volume element, $d\tau_J$, corresponding to the given curvilinear coordinates (see Eq. 1b). It is worth noting that (i) when $n<3N$, the system is subjected to constraints as, for instance, in the case of reduced-dimensionality models. (ii) when $n=3N$, the system is, of course, not constrained and, in addition, $J(\boldsymbol{Q})$ is the Jacobian determinant for changing from 3*N* Laboratory-Fixed Cartesian coordinates

to 3*N* curvilinear coordinates (for more details see, for instance, ref [5]), in which case the volume element is Euclidean.

In most cases, the volume element, $d\tau_J$, is not adapted to the basis set into which the wave function is to be expanded. Indeed, the choice of a set of orthonormal basis functions very often requires to define a new volume element, $d\tau_\rho = \rho(\boldsymbol{Q})dQ^1 \cdots dQ^n$ (Eq. 2e), where $\rho(\boldsymbol{Q})$ is a (real positive) weight function. In that case, which may also be regarded as a change in the normalization convention of the wave functions, the corresponding KEO has to be modified[1][2][3][4][5][19] as follows:

$$\hat{T}_\rho(\boldsymbol{Q}, \partial_{\boldsymbol{Q}}) = \sqrt{\frac{J(\boldsymbol{Q})}{\rho(\boldsymbol{Q})}}\hat{T}_J(\boldsymbol{Q}, \partial_{\boldsymbol{Q}})\sqrt{\frac{\rho(\boldsymbol{Q})}{J(\boldsymbol{Q})}} \quad \text{Eq. 2a}$$

$$= -\frac{\hbar^2}{2}\sqrt{\frac{J(\boldsymbol{Q})}{\rho(\boldsymbol{Q})}}\frac{1}{J(\boldsymbol{Q})}\sum_{i=1}^{n}\frac{\partial.}{\partial Q^i}\,J(\boldsymbol{Q})\sum_{j=1}^{n}G^{ij}(\boldsymbol{Q})\frac{\partial.}{\partial Q^j}\,\sqrt{\frac{\rho(\boldsymbol{Q})}{J(\boldsymbol{Q})}} \quad \text{Eq. 2b}$$

$$= -\frac{\hbar^2}{2}\frac{1}{\rho(\boldsymbol{Q})}\sum_{i=1}^{n}\frac{\partial.}{\partial Q^i}\,\rho(\boldsymbol{Q})\sum_{j=1}^{n}G^{ij}(\boldsymbol{Q})\frac{\partial.}{\partial Q^j} + V_{ep}(\boldsymbol{Q}) \quad \text{Eq. 2c}$$

$$= \sum_{i\geq j}^{n} f_2^{ij}(\boldsymbol{Q})\frac{\partial^2.}{\partial Q^i \partial Q^j} + \sum_{i}^{n} f_1^{i}(\boldsymbol{Q})\frac{\partial.}{\partial Q^i} + V_{ep}(\boldsymbol{Q}) \quad \text{Eq. 2d}$$

and $d\tau_\rho = \rho(\boldsymbol{Q})dQ^1 \cdots dQ^n$ Eq. 2e

The derivation of Eq. 2d has been known for many years. [4][5][9][10][11][12][13][14] However, to be complete and to ease the analysis of the complexity in terms of numerical operations (multiplications), an overview of the derivation of Eq. 2d is given in the appendix A.

As mentioned above, curvilinear coordinates are essential to compute ro-vibrational levels and to propagate wave packets of a molecular system efficiently. The numerical procedures for the time-dependent approach (Chebychev [20], Runge-Kutta , Taylor expansion [21]) or the time-independent approach (iterative diagonalization techniques, such as Davidson [22][23] or

Lanczos [24]), require repeated computation of the action of the potential and the KEO on a wave function or a wave packet.

When the number of degrees of freedom, n, is small (n<10) either for small systems (tetra or penta-atomic molecules) or for reduced dimensionality models, the numerical approach is efficient and easy to implement for treating the action of the KEO (as given by Eq. 2d) on a wave function. However, when the number of degrees of freedom is large, this numerical approach has to face two limitations:

(i) The number of terms becomes very large (i.e. the number of $f_2^{ij}(\boldsymbol{Q})$, $f_1^i(\boldsymbol{Q})$ and $V_{ep}(\boldsymbol{Q})$) in the KEO (Eq. 2d) is about $n^2/2$ (more precisely, $(n+1)(n+2)/2$), and each term has to be computed and stored on the full grid. So, in our previous study on methanol in 12D [15], the KEO is composed of 91 terms and for the largest calculation, the number of grid points was about 0.9 billion. On our computer, the KEO on the full grid could not be stored in memory (about 605 GB) and was therefore stored on a disk.

(ii) The numerical calculation of the KEO can be time-consuming. Indeed, the computations of $f_2^{ij}(\boldsymbol{Q})$, $f_1^i(\boldsymbol{Q})$ and $V_{ep}(\boldsymbol{Q})$ scale as n^3, n^4 and n^5, respectively (see appendix A for the expressions of these terms (Eq. A1) and a discussion of their numerical cost).

So, for instance, with a 12-core computer, about 9 days were needed to calculate the Hamiltonian (potential and KEO) on the full grid for the largest calculation of our previous 12D study on methanol.

Difficulties of the same kind are also present in the standard DVR approach where usually Eq. 2c is used [25][13], instead of Eq. 2d, where the number of terms to be stored on the full grid is also about $n^2/2$ and where the $V_{ep}(\boldsymbol{Q})$ has also to be calculated.

The unfavorable scaling (n^5) of $V_{ep}(\boldsymbol{Q})$ and the large number of terms in the KEO's prevent an efficient use of the numerical kinetic energy operator for systems with a large number of degrees of freedom.

The main objective of the present work is to show that the use of a numerical approach is possible without storing the full on-the-grid KEO in memory or on disk, provided that the KEO is *repeatedly computed on-the-fly i.e.* each time the KEO action on a wave function is required. In addition, we will show that the unfavorable (n^5) scaling of $V_{ep}(\boldsymbol{Q})$ *can be avoided* by using Eq. 2b directly [26].

II KEO action on a wave function

The action of the KEO, $\hat{T}_\rho\left(\boldsymbol{Q}, \partial_{\boldsymbol{Q}}\right)$, on a wave function, $\Psi(\boldsymbol{Q})$, is the most time-consuming part of the quantum dynamics approaches (time-dependent or time-independent). Several steps are required to perform this operation: (i) Calculation of the derivatives (first and second order) of a wave function known on the grid (ii) taking into account the kinetic energy terms (the $f_2^{ij}(\boldsymbol{Q})$, $f_1^i(\boldsymbol{Q})$ and $V_{ep}(\boldsymbol{Q})$ for Eq. 2d or $G^{ij}(\boldsymbol{Q})$ and $V_{ep}(\boldsymbol{Q})$ for Eq. 2c).

IIa) derivatives of a wave function:

Here, we assume that the wave function, $\Psi(\boldsymbol{Q})$, is known on the full grid, *i.e.* this wave function is expressed as a column vector, $\begin{bmatrix} \vdots \\ \Psi(\boldsymbol{Q_U}) \\ \vdots \end{bmatrix}$, where $\boldsymbol{Q_U}$ is the value of the n coordinates for the $\boldsymbol{U}^{\text{th}}$ grid point and U runs from 1 to the total number, NQ. Then, to calculate its derivatives, $\partial_i\Psi = \frac{\partial\Psi}{\partial Q^i}$, with respect to coordinate Q^i on the full grid, we have to compute $\frac{\partial\Psi}{\partial Q^i}$ for all $\boldsymbol{Q_U}$ points and it will be noted as a column vector, $\begin{bmatrix} \vdots \\ \partial_i\Psi(\boldsymbol{Q_U}) \\ \vdots \end{bmatrix}$.

To simplify the discussion, let assume that the wave function has two coordinates only, x and y, and is expressed as a direct product with nq_x and nq_y grid points along the x and y coordinates, respectively (see also the discussion in the review by Light and Carrington on the DVR approach [25]). The wave function is thus represented on the 2D-grid as a matrix, $\Psi^{gg}(u_x, u_y)$, where the double upper index, gg, means that Ψ is expanded on the grid for both coordinates, x and y. The indices, u_x and u_y, run from one to nq_x and nq_y grid points, respectively.

To compute the derivative with respect to x, $\partial_x\Psi = \frac{\partial\Psi}{\partial x}$, the wave function has to be partially expanded on the orthonormal basis set, $\boldsymbol{B}^x$, associated to the coordinate, x. This 1D-basis-set is composed of nb_x basis functions: $\left[B_1^x(x) \quad \cdots \quad B_{k_x}^x(x) \quad \cdots \quad B_{nb_x}^x(x)\right]$. This wave

function, $\Psi^{bg}(k_x, u_y)$, where the upper indices are b (for the basis expansion on x) and g (for the grid expansion on y), is given by:

$$\Psi^{bg}(k_x, u_y) = \sum_{u_x=1}^{nq_x} \Psi^{gg}(u_x, u_y) \cdot B_{k_x}^{x}(u_x) \cdot \omega_x(u_x) \quad \text{Eq. 3a}$$

$$\partial_x \Psi^{gg}(u_x, u_y) = \sum_{k_x=1}^{nb_x} \Psi^{bg}(k_x, u_y) \cdot \partial_x B_{k_x}^{x}(u_x) \quad \text{Eq. 3b}$$

The first equation (Eq. 3a) is simply the partial integration over x of the product $\left(B_{k_x}^{x}(x) \cdot \Psi(x, y)\right)$ computed by means of a Gaussian quadrature. In Eq. 3a, the $\omega_x(u_x)$ are the weights associated to the grid point u_x. Next, the $\Psi^{bg}(k_x, u_y)$, is transformed back on the grid (Eq. 3b), but taking into account the derivative with respect to x, hence, the use of $\partial_x B_{k_x}^{x}(u_x)$.

These two transformations can be merged into a single one using a square matrix, $\boldsymbol{D}_x^{(1)}$ (size $nq_x.nq_x$), which represents the first derivative operator in x. A similar procedure is also used in the well-known FBR-DVR approaches, where, $\sqrt{\omega_x(u_x)}$ is taken into account in $B_{k_x}^{x}(u_x)$ and $\partial_x B_{k_x}^{x}(u_x)$ (see ref [25]). Furthermore, our approach can be easily modified when second order derivatives are required (one has then to use $\partial_{xx} B_{k_x}^{x}(u_x)$ instead of $\partial_x B_{k_x}^{x}(u_x)$) and the matrix representation is noted $\boldsymbol{D}_x^{(2}$. Of course, it can be extended to systems with more than two degrees of freedom. In that case, the coordinate y and its corresponding index, u_y, have to be viewed as a collective coordinate and a collective index, respectively. Furthermore, this matrix, $\boldsymbol{D}_x^{(1)}$, can be obtained using a pseudoinverse procedure,[27] which is numerically more stable when nb_x is much smaller than nq_x and in particular when a contracted basis set is used (see the appendix B, for an explanation of the procedure).

IIb) KEO action:

In the previous subsection, we have briefly recalled how to compute the first derivatives,

$\partial_i\Psi = \frac{\partial\Psi}{\partial Q^i}$, and second derivatives, $\partial_{ij}\Psi = \frac{\partial^2\Psi}{\partial Q^i \partial Q^j}$, of a wave function on the full grid. In other words, we know the following column vectors:

$$\boldsymbol{\Psi} = \begin{bmatrix} \vdots \\ \Psi(\boldsymbol{Q_U}) \\ \vdots \end{bmatrix}, \quad \partial_i\boldsymbol{\Psi} = \begin{bmatrix} \vdots \\ \partial_i\Psi(\boldsymbol{Q_U}) \\ \vdots \end{bmatrix}, \quad \partial_{ij}\boldsymbol{\Psi} = \begin{bmatrix} \vdots \\ \partial_{ij}\Psi(\boldsymbol{Q_U}) \\ \vdots \end{bmatrix} \qquad \text{Eq. 4}$$

where, $\boldsymbol{Q_U}$ is the value of the n coordinates for the $\boldsymbol{U}^{\text{th}}$ grid point. Thus, on the grid, the KEO action on $\boldsymbol{\Psi}$ gives a new vector, $\boldsymbol{\chi}$:

$$\boldsymbol{\chi} = \begin{bmatrix} \vdots \\ \chi(\boldsymbol{Q_U}) \\ \vdots \end{bmatrix} = \sum_{i\geq j}^{n} \begin{bmatrix} \vdots \\ f_2^{ij}(\boldsymbol{Q_U})\partial_{ij}\Psi(\boldsymbol{Q_U}) \\ \vdots \end{bmatrix} + \sum_{i}^{n} \begin{bmatrix} \vdots \\ f_1^{i}(\boldsymbol{Q_U})\,\partial_i\Psi(\boldsymbol{Q_U}) \\ \vdots \end{bmatrix} + \begin{bmatrix} \vdots \\ V_{ep}(\boldsymbol{Q_U})\Psi(\boldsymbol{Q_U}) \\ \vdots \end{bmatrix} \qquad \text{Eq. 5}$$

This is close to the procedure used to calculate the action of a potential function on a wave function in the standard FBR-DVR approach [25][13], yet more terms being present here.

It is worth noting, that, when the full KEO-vectors ($f_2^{ij}(\boldsymbol{Q_U})$, $f_1^{i}(\boldsymbol{Q_U})$ and $V_{ep}(\boldsymbol{Q}_u)$), can be stored in memory, these operations are very fast because everything is known on the grid. However, when it is not possible to store them in memory, we can calculate them on-the-fly, but this too will be time-consuming for large systems due to the n^5 scaling of $V_{ep}(\boldsymbol{Q}_u)$, and therefore unrealistic.

To circumvent those difficulties, we now show that Eq. 2b can be used, directly and easily, instead of Eqs. 2c or 2d (see ref [26]) and so, in particular, that the computation of the extra-potential term can be avoided.

The following steps are required, starting from the right-hand side of Eq. 2b:

(i) Multiplication by $\sqrt{\rho(\boldsymbol{Q})/J(\boldsymbol{Q})}$:

$$\boldsymbol{\chi_1} = \begin{bmatrix} \vdots \\ \chi_1(\boldsymbol{Q_U}) \\ \vdots \end{bmatrix} = \begin{bmatrix} \vdots \\ \sqrt{\rho(\boldsymbol{Q_U})/J(\boldsymbol{Q_U})}\,\Psi(\boldsymbol{Q_U}) \\ \vdots \end{bmatrix} \qquad \text{Eq. 6}$$

(ii) Differentiation with respect to Q^j: we use the procedure of the previous subsection on $\boldsymbol{\chi}_1$, to get $\partial_j \boldsymbol{\chi}_1$.

(iii) Multiplication by $G^{ij}(\boldsymbol{Q})$, summation over j and multiplication by $J(\boldsymbol{Q_U})$:

$$\boldsymbol{\chi}_{2i} = \begin{bmatrix} \vdots \\ \chi_{2i}(\boldsymbol{Q_U}) \\ \vdots \end{bmatrix} = \begin{bmatrix} \vdots \\ J(\boldsymbol{Q_U}) \sum_{j=1}^{n} G^{ij}(\boldsymbol{Q_U}) \cdot \partial_j \boldsymbol{\chi}_1(\boldsymbol{Q_U}) \\ \vdots \end{bmatrix} \quad \text{Eq. 7}$$

For large systems, $G^{ij}(\boldsymbol{Q_U})$ is calculated on-the-fly, **but only once,** for all vectors $\boldsymbol{\chi}_{2i}$. So, for instance, during the block-Davidson procedure, the $\boldsymbol{G}$ matrix is re-computed for each iteration.

(iv) Differentiation of $\boldsymbol{\chi}_{2i}$ with respect to Q^i, by means of the procedure given in the previous subsection, to get $\partial_i \boldsymbol{\chi}_{2i}$.

(v) Summation over i and multiplication by $-\hbar^2/\sqrt{4J(\boldsymbol{Q})\rho(\boldsymbol{Q})}$ to get the full action of the KEO on the wave function:

$$\boldsymbol{\chi} = \begin{bmatrix} \vdots \\ \chi(\boldsymbol{Q_U}) \\ \vdots \end{bmatrix} = \begin{bmatrix} \vdots \\ -\hbar^2/\sqrt{4J(\boldsymbol{Q_U})\rho(\boldsymbol{Q_U})} \sum_{i=1}^{n} \partial_i \chi_{2i}(\boldsymbol{Q_U}) \\ \vdots \end{bmatrix} \quad \text{Eq. 8}$$

In this approach, we need to compute only the metric tensor, $\boldsymbol{G}(\boldsymbol{Q})$, and $J(\boldsymbol{Q})$. There is no need to compute the extrapotential term, V_{ep}, anymore, which is one of the main differences with the standard-DVR approaches previously implemented, where Eq. 2c is used instead of Eq. 2b, so that the action of the extrapotential term, V_{ep}, on the wave function has to be calculated.

Furthermore, and since the calculation of $\boldsymbol{G}(\boldsymbol{Q})$ scales as n^3, it is possible to compute it with an on-the-fly procedure i.e. without storing it in memory on the full grid.

In the present procedure and for a single wave function, we need the following vectors on the full grid (Ψ or $\boldsymbol{\chi}_1$ or $\boldsymbol{\chi}$, $\partial_j\boldsymbol{\chi}_1$, $\partial_i\boldsymbol{\chi}_{2i}$ and $\mathbf{J}$, $\boldsymbol{\rho}$) and one more vector for the potential. Altogether, we need $2n$+4 vectors on the full grid, whereas, in our previous implementation, about $n^2/2$ vectors were required.

III Application to methanol

In the present paper, we have used the same potential [28] as in our previous study. [15] The coordinates are defined as a series of transformations between coordinate sets [15] (see figure 1) and are given as follows: (i) *z-matrix coordinates,* Q_{zmat}: the first set of curvilinear coordinates is defined through a z-matrix (fig. 1). The corresponding transformation relates the Cartesian coordinates to z-matrix ones, Q_{zmat}. (ii) *linear transformation, giving* Q_{sym}: the three dihedral angles associated to the hydrogen of the methyl group of the z-matrix, φ_1, φ_2 and φ_3 are combined to give three angles, ϕ_a, ϕ_{e1} and ϕ_{e2} (see fig. 1). The torsion of the methyl group with respect to the OH bond is given by the first angle ϕ_a. This transformation is essential to preserve the symmetry of the molecule, [29][30]. (iii) *flexible coordinates,* Q_{flex}: the i^{th} flexible coordinates, Q^i_{flex} is given by $Q^i_{sym} - Q^i_{opt}(\phi_a)$, where $Q^i_{opt}(\phi_a)$ is the optimal value of the Q^i_{sym} coordinates along the torsional path (in ϕ_a). Furthermore, these optimal values are expanded in Fourier series, using the three equivalent minima and three equivalent transition states. (iv) *curvilinear normal modes,* Q_{NM}: these coordinates are defined as a constant linear transformation between 11-flexible ones (all coordinates except ϕ_a). The 11x11 hessian and kinetic matrices used to get the curvilinear normal modes are obtained from averaging hessian and kinetic matrices at the three equivalent minima.

Fig 1: Coordinate definitions adapted to the symmetry and reducing the coupling between modes.

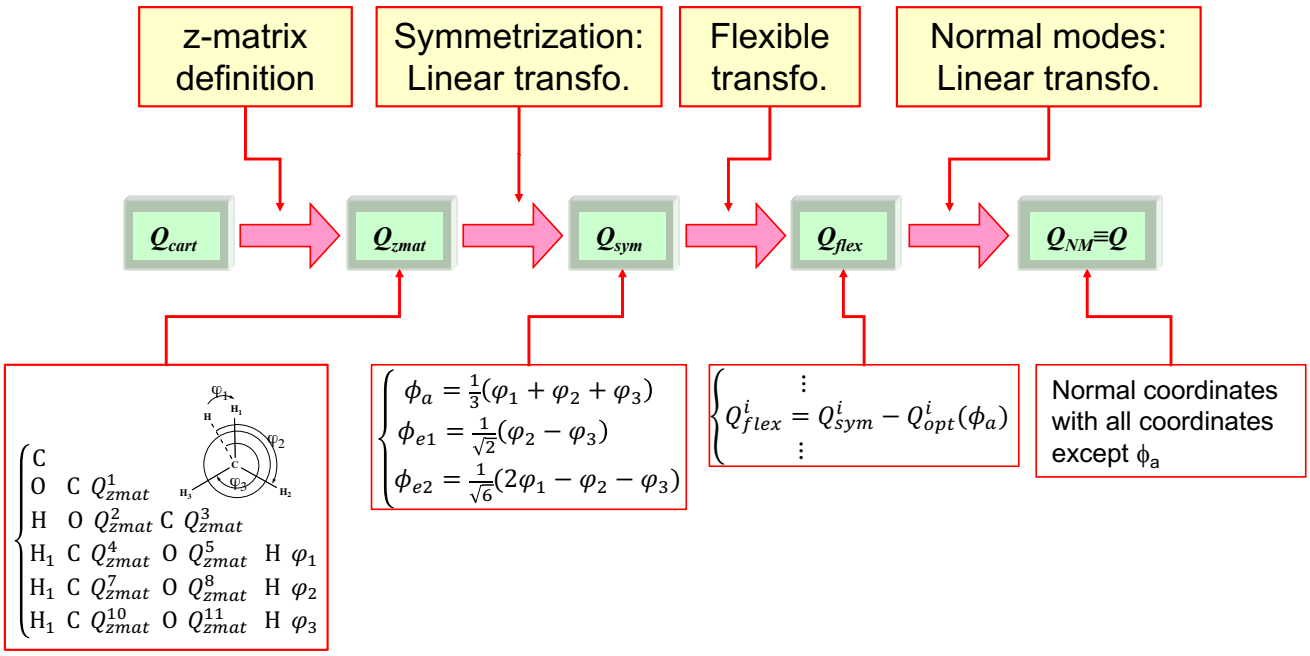

It is important to note that, at the end of all these transformations, the coordinates used in the dynamics are closely related to coordinates associated with a reaction path Hamiltonian, RPH, or similar approaches in which the curvilinear normal modes evolve along the path. However, in our previous [15] and in the present studies, the curvilinear normal modes remain constant along the torsional mode. This simplified RPH version does not prevent from performing exact quantum calculation for a given potential.

Furthermore, the full 12D-basis set is expressed as a direct product of (i) a 1D-contracted basis set for the torsion, made of 24 eigenfunctions obtained from the diagonalization of a 1D-Hamiltonian. The uncontracted basis set is made of 36 sine and cosine functions and the numerical integrations were performed using 48 quadrature grid points. (ii) a 11D-Smolyak basis set for the other coordinates. More precisely, the K^{th} 11D-basis functions, $B_K^{11D}(\boldsymbol{Q})$, is defined as a product of 11 Harmonic Oscillator basis functions as follows:

$$B_K^{11D}(\boldsymbol{Q}) = B_{k_1}^1(Q^1) \dots B_{k_i}^i(Q^i) \dots B_{k_{11}}^{11}(Q^{11}) \qquad \text{Eq. 8}$$

where $B^{i}_{k_i}(Q^i)$ is the k_i^{th} Harmonic Oscillator basis function associated with the i^{th} coordinate, Q^i. Then, the $B_K^{11D}(\boldsymbol{Q})$ are selected by means of the parameters, ℓ_i and L_B, such as $0 \leq \sum_{i=1}^{11} \ell_i \leq L_B$ and a relation (for all i) between the ℓ_i and the k_i given in the following table (table 1):

Table 1: relation between the k_i, the ℓ_i and nb_i for all values of index i.

k_i	1	2	3 4	5 **6** 7	8 ... **11**	12 ... 16	17 ... 22	23 ... 29	30 ...37
nb_i	1	2	4	7	11	16	22	29	37
ℓ_i	0	1	2	**3**	**4**	5	6	7	8

For instance, for a given 11D-basis function defined with this set of k_i, $[k_1 \dots k_i \dots k_{11}] = [1, 1, \mathbf{6}, 1, \mathbf{11}, 1, 1, 1, 1, 1, 1]$, the ℓ_i set is $[\ell_1 \dots \ell_i \dots \ell_{11}] = [0, 0, \mathbf{3}, 0, \mathbf{4}, 0, 0, 0, 0, 0, 0]$ and the sum of the ℓ_i is 7. Therefore, if the parameter L_B, which defines the size of the basis set is equal or larger than 7, this 11D-basis function is kept and otherwise it is discarded. It is important to note for example, that if k_3=7 (instead of 6), the value of ℓ_3 remains the same (3). In a certain way and for each index i, the ℓ_i define the number of basis functions, nb_i, such as $nb_i(\ell_i) = nb_i(\ell_i - 1) + \ell_i$ and $nb_i(0) = 1$ (see table 1). This kind of selection is similar to the pruned basis set of Carrington's group [31][32]. With this non-direct product basis set, a Smolyak sparse grid can be used[33][34][35][36][15]; the grid size is determined by means of a Smolyak parameter, L_G, defined as L_G=L_B+1 and the number of quadrature grid points for each HO basis set is $nq_i(\ell_i) = nq_i(\ell_i - 1) + \ell_i$. To converge the energy levels within 0.01 cm^{-1}, the values of L_B and L_G are 7 and 8, respectively.

In our previous study,[15] the Smolyak basis set was defined in a slightly different way *i.e.* $nb_i(\ell_i) = nb_i(\ell_i - 1) + 1$ and $nq_i(\ell_i) = nq_i(\ell_i - 1) + 1$. Therefore, L_B and L_G had to be larger (L_B=9 and L_G=10) than those of the present study in order to converge the energy levels. However, in both studies, the basis set size (NB) and the number of grid points (NQ) are of the same order of magnitude (see table 2).

It is important to note that the diagonalization was performed using a block Davidson procedure [23]. However, during the Davidson iterations and with the present approach, the intermediate Hamiltonian matrix is not Hermitian (due to the numerical approximation of the differentiation in the steps ii and iv of the KEO action). This is why we have used a Lapack subroutine to diagonalize this non-symmetric matrix.

In table 2, we present some torsional energy levels from the present study and from our previous ones. The comparison is almost perfect; the energy differences are not larger than 0.01 cm^{-1} for all levels. Furthermore, due to the symmetry, some levels are degenerate (those corresponding to the following experimental values: 9.1, 208.9, 510.3 and 751.0 cm^{-1}) and the computed energy components are not strictly equal due to approximations in the numerical integration. However, the largest difference between the two components is only 0.005 cm^{-1} for the level at 741.78 cm^{-1}. It will be noted that in our previous study, this was not possible (because it required too much time), except for the zero-point energy (ZPE) to obtain the energy levels, for the largest calculation (L_B=9, L_G=10), which already took 20 days. Now with the present approach, in which the metric tensor is computed for each Hamiltonian operator action on a wave function, the calculation takes only 8 days for all the treated states. Furthermore, and as expected, the memory requirement is much smaller (about five times), for grids of similar sizes.

Table 2: First column, torsional energy levels (in cm^{-1}) of methanol; second column, experimental levels; third and fourth columns, levels and parameters from our previous study [15]; fifth and sixth columns, levels and parameters from the present work using ELVIBROT. The levels at 9.1, 208.9, 510.3 and 751.0 are degenerate.

	Exp.	ELVIBROT previous work		ELVIBROT present work	
	Exp.	L_B=6, L_G=8	L_B=9, L_G=10	L_B=6, L_G=7	L_B=7, L_G=8
Energy levels	/	11088.76	11088.50	11088.55	11088.51
	9.1	9.14, 9.15		9.15	9.15
	208.9	205.34		205.34	205.34
	294.7	290.69		290.69	290.69
	353.0	347.49		347.49	347.49
	510.3	503.54		503.53	503.53
	751.0	741.80		741.78	741.78
Basis set size: NB	/	297 024	4 031 040	920 064	3 196 008
Grid size: NQ	/	88 584 912	892 360 032	134 737 200	588 600 720
Memory requirement	/	60 GB	605 GB on disk	28 GB	123 GB

VI Conclusion and perspectives

From a numerical point of view, the approach developed in the present paper opens the way to using sophisticated coordinates with a numerical *on-the-fly* KEO for large systems without introducing approximations [37][38] (such as using constant or Taylor-expanded metric tensors or neglecting the extra-potential term). Indeed, we show that the numerical procedure implemented here enables to reproduce the previous results exactly [15] with less computational resources (memory and cpu time).

However, that the memory scales as $2n$ (n being the number of degrees of freedom) is clearly a limitation, although not as strong as the $n^2/2$ scaling in our previous implementation. To address this problem, one can use the data structure of the Smolyak representation (the sum of small direct product bases or grids) in order to avoid almost completely, except for the potential, to store vectors on the full grid. In other words, we need to merge the Smolyak scheme with the *on-the-fly* numerical action of the KEO's on the wave functions.

There is also another issue worth analyzing in more detail. Indeed, in order to deal with operators such as $\frac{\partial}{\partial x}$, the use of $\boldsymbol{D}_x^{(1)}$ (obtained from Eq. 3) may give rise to a non-Hermitian Hamiltonian matrix [39][25] when $\frac{\partial .}{\partial Q^i}$ (Eq. 2b or Eq. 2c), is applied. Unfortunately, when using (Eq. 2b or Eq. 2c), the non-hermiticity cannot be reduced by increasing the number of grid points as usual. For the calculation of eigenlevels, the use of a diagonalization procedure for non-symmetric matrices solves this problem, although some spurious eigenvectors may crop up, which can be easily discarded upon inspection. Furthermore, the consequences of the loss of hermiticity of the Hamiltonian operators during the time-dependent approach are not clear. One might probably try differentiation on the left $\frac{\overleftarrow{\partial .}}{\partial Q^i}$ [39] instead of the usual differentiation on the right, $\frac{\partial .}{\partial Q^i}$.

Moreover, it is worth pointing out that this non-hermicity issue is almost absent when all derivative operators act directly on the wave function (Eq. 2d). More precisely, the Hamiltonian matrix may be slightly non-Hermitian, but this can be numerically suppressed, by increasing the number of grid points without increasing the number of basis functions.

Anyway, and whatever the remaining difficulties, *numerical on-the-fly* implementations as developed in the present paper, will certainly contribute to open the way to rigorous quantum computations of systems with many degrees of freedom.

Acknowledgements

One of us (DL) gratefully acknowledges the hospitality of the School of Physics and the Institute of Condensed Matter and Nanosciences (NAPS) of the Université Catholique de Louvain, where part of the present work was carried out.

Appendix

A) Derivation of the KEO and its numerical cost:

The derivation of the numerical kinetic energy operator has been known for many years and there are several ways to obtain the expression given in Eq. 2d. [4][5][9][10][11][12][13][14] In the present study, the $\boldsymbol{x}(\boldsymbol{Q})$ approach is used, where $\boldsymbol{Q}$ is the set of n curvilinear coordinates and $\boldsymbol{x}$ is the set of Cartesian coordinates and in this case the $f_2^{ij}(\boldsymbol{Q})$, $f_1^i(\boldsymbol{Q})$ and $V_{ep}(\boldsymbol{Q})$ are given by the following expressions:

$$f_2^{ij}(\boldsymbol{Q}) = \begin{cases} -\frac{\hbar^2}{2} G^{ij}(\boldsymbol{Q}) & \text{for i = j} \\ -\hbar^2 G^{ij}(\boldsymbol{Q}) & \text{for i} > j \end{cases} \qquad \text{Eq. A1a}$$

$$f_1^i(\boldsymbol{Q}) = \left(\sum_{j=1}^{n} \frac{\partial G^{ij}(\boldsymbol{Q})}{\partial Q^j} + G^{ij}(\boldsymbol{Q}) \frac{\partial \rho(\boldsymbol{Q})}{\partial Q^j} \frac{1}{\rho(\boldsymbol{Q})} \right) \qquad \text{Eq. A1b}$$

Eq. A1c

$$V_{ep}(\boldsymbol{Q}) = \frac{1}{8}\sum_{i,j=1}^{n} G^{ij}(\boldsymbol{Q})\left[\frac{\partial\rho(\boldsymbol{Q})}{\partial Q^i}\frac{1}{\rho(\boldsymbol{Q})}\frac{\partial\rho(\boldsymbol{Q})}{\partial Q^j}\frac{1}{\rho(\boldsymbol{Q})} - \frac{\partial J(\boldsymbol{Q})}{\partial Q^i}\frac{1}{J(\boldsymbol{Q})}\frac{\partial J(\boldsymbol{Q})}{\partial Q^j}\frac{1}{J(\boldsymbol{Q})}\right]$$
$$+\frac{1}{4}\sum_{i,j=1}^{n}\frac{\partial G^{ij}(\boldsymbol{Q})}{\partial Q^j}\left[\frac{\partial J(\boldsymbol{Q})}{\partial Q^i}\frac{1}{J(\boldsymbol{Q})} - \frac{\partial\rho(\boldsymbol{Q})}{\partial Q^i}\frac{1}{\rho(\boldsymbol{Q})}\right]$$
$$+\frac{1}{4}\sum_{i,j=1}^{n} G^{ij}(\boldsymbol{Q})\left[\frac{\partial^2 J(\boldsymbol{Q})}{\partial Q^i\partial Q^j}\frac{1}{J(\boldsymbol{Q})} - \frac{\partial^2\rho(\boldsymbol{Q})}{\partial Q^i\partial Q^j}\frac{1}{\rho(\boldsymbol{Q})}\right]$$

The key ingredients are the contravariant components of the metric tensor, $G^{ij}(\boldsymbol{Q})$. Its matrix representation, $\boldsymbol{G}$ can be obtained as follows:

$$\boldsymbol{G} = \left[G^{ij}(\boldsymbol{Q})\right] = \left[g_{ij}(\boldsymbol{Q})\right]^{-1} \qquad \text{Eq. A2}$$
($i,j = 1, ...n$)

where, $g_{ij}(\boldsymbol{Q})$ are the covariant components of the metric tensor, associated to the matrix, $\boldsymbol{g}$, with

$$g_{ij}(\boldsymbol{Q}) = \sum_{\lambda=1}^{3N} m_\lambda \frac{\partial x^\lambda(\boldsymbol{Q})}{\partial Q^i}\frac{\partial x^\lambda(\boldsymbol{Q})}{\partial Q^j} \qquad \text{Eq. A3}$$

In the previous equation, N is the number of atoms and m_λ is the atomic mass associated with the λ^{th} Cartesian coordinates. Furthermore, when all degrees of freedom are considered (no constraints), n is equal to $3N$.
From the two previous equations, one can see that the number of operations (i.e. multiplications) to build the $\boldsymbol{G}$ matrix and therefore the f_2^{ij} terms (Eq. A1a), scales as O(n^3): indeed, $6N$ operations to build each of the n^2 component, g_{ij} (Eq. A3), and about n^3 operations for the matrix inversion (Eq. A2).

Next, to compute the f_1^i, one needs several ingredients: (i) the $\boldsymbol{G}$ matrix which is already known. (ii) $\rho(\boldsymbol{Q})$, the weight function associated with the chosen volume element and the derivative of $\rho(\boldsymbol{Q})$. In all applications, the expression of $\rho(\boldsymbol{Q})$ is really simple (product of 1D-functions). Therefore, the numerical cost associated to the $\rho(\boldsymbol{Q})$ contributions is small. (iii) the n first derivatives of the $\boldsymbol{G}$ matrix, which are the costly contributions (see Eqs. A4, A5).

The derivation of the $\boldsymbol{G}$ matrix reads:

$$\frac{\partial \boldsymbol{G}}{\partial Q^k} = -\boldsymbol{G}\frac{\partial \boldsymbol{g}}{\partial Q^k}\boldsymbol{G} \qquad \text{Eq. A4}$$

(k = 1, ...n)

and the n derivatives of the components of $\boldsymbol{g}$ are obtained through the differentiation of Eq. A.3 and are given as follows:

$$\frac{\partial g_{ij}(\boldsymbol{Q})}{\partial Q^k} = \sum_{\lambda=1}^{3N} m_\lambda \left[\frac{\partial^2 x^\lambda(\boldsymbol{Q})}{\partial Q^k \partial Q^i}\frac{\partial x^\lambda(\boldsymbol{Q})}{\partial Q^j} + \frac{\partial x^\lambda(\boldsymbol{Q})}{\partial Q^i}\frac{\partial^2 x^\lambda(\boldsymbol{Q})}{\partial Q^k \partial Q^j}\right] \qquad \text{Eq. A5}$$

From the previous equations, one can see that the number of operations scales (i) as $2n^4$: $2n$ matrix multiplications (n^3 operations) for the n derivatives for Eq. A4. (ii) as 3x3N for each term $\frac{\partial g_{ij}(\boldsymbol{Q})}{\partial Q^k}$ (n^3 terms).
Therefore, the numerical cost to get all the f_1^i scales as O(n^4).

The computation of the extrapotential term, $V_{ep}(\boldsymbol{Q})$, is the costliest among the Eq. A1 terms. Indeed, all elements from Eq. A1c are already known, except those implying $J(\boldsymbol{Q})$ and its first and second derivatives with respect to the curvilinear coordinates. $J(\boldsymbol{Q})$ is expressed as a function of the determinant of $\boldsymbol{g}$ as follows:

$$J(\boldsymbol{Q}) = \sqrt{\det(\boldsymbol{g})} \qquad \text{Eq. A6}$$

The numerical cost scales as O(n^3), for det($\boldsymbol{g}$). Furthermore, the computation of the first and the second derivatives of $J(\boldsymbol{Q})$ requires, respectively, the first (Eq. A5) and the second (obtained from the differentiations of Eq. 5 with respect to Q^ℓ))- derivatives of $\boldsymbol{g}$. Thus, for all i and j values, the numerical cost of $\frac{\partial^2 g(\boldsymbol{Q})}{\partial Q^i \partial Q^i}$ and $\frac{\partial^2 J(\boldsymbol{Q})}{\partial Q^i \partial Q^j}$ scale as O(n^5).
Therefore, the numerical cost to get the $V_{ep}(\boldsymbol{Q})$ scales as O(n^5).

The method developed in the present paper is valid for the quantum treatment of any system with n degrees of freedom. It goes without saying that it can be used in the particular case of a N-atom molecular system (constrained n<3N or not constrained n=3N) by introducing the following n generalized coordinates $\boldsymbol{Q} = [\boldsymbol{q}, \boldsymbol{\Theta}, \boldsymbol{X_{CM}}]$, where $\boldsymbol{q} = [q^1 \cdots q^{n-6}]$ are internal (shape) coordinates, $\boldsymbol{\Theta}$ are the three Euler angles that orient a Body-fixed frame with respect to the Space-fixed frame and $\boldsymbol{X_{CM}}$ are the three Cartesian coordinates that determine the position of the center of mass of the molecular system in the Laboratory-fixed frame.

B) Derivatives of a wave function, pseudoinverse procedure:

The procedure described in section IIa (Eq. 3) works well in most cases and, when the numbers of basis function, *nb*, and grid points, *nq*, are equal, this procedure is equivalent to the one used in the DVR approach. However, in some circumstances and in particular for contracted basis sets, the numerical precision of the matrix representation on the grid of the first, $\boldsymbol{D}_x^{(1)}$, and second, $\boldsymbol{D}_x^{(2)}$, derivative operators is not satisfactory.

To show this feature, we will compute the differences between the direct computation of the first derivative of the k^{th} basis function $B_k(x)$ at a given point x_u, $\left.\frac{\partial B_k(x)}{\partial x}\right|_{x_u} = \partial_x B_k(x_u)$ using the usual relations of the orthogonal polynomials or the basis functions and the two numerical approaches, the standard one using Eq. 3 and another one using a pseudoinverse procedure. [27]

Both approaches proceed in two steps, the second one is the same in both cases and corresponds to Eq. 3b, while in the first step, a vector known on the grid, $\Psi^g = \begin{bmatrix} \vdots \\ \Psi(x_u) \\ \vdots \end{bmatrix}$, (with *nq* grid points) is projected onto the *nb* basis functions, $\Psi^b = \begin{bmatrix} \vdots \\ \mathrm{C}_k \\ \vdots \end{bmatrix}$, (the upper indices *b* and *g* stand, respectively, for the basis expansion and for the grid expansion) as follows:

$$\Psi^b = \boldsymbol{M}^{bg} \cdot \Psi^g \qquad \text{Eq. A7}$$

where $\boldsymbol{M}^{bg}$ is a matrix (size *nb.nq*), which is computed by using two different procedures:
(i) In the standard approach, $\boldsymbol{M}^{bg}$ is given as in Eq. 3a ($\boldsymbol{M}^{bg}(k,u) = B_k(x_u) \cdot \omega_x(u)$).
(ii) In the pseudoinverse approach, $\boldsymbol{M}^{bg}$ is obtained from solving a system of linear equations, where the k^{th}-basis function on the grid, $\begin{bmatrix} \vdots \\ \mathrm{B}_k(x_u) \\ \vdots \end{bmatrix}$, is Ψ^g so that the corresponding, Ψ^b, is a vector for which all components are zero except C_k, which is equal to one. All vectors $\begin{bmatrix} \vdots \\ \mathrm{B}_k(x_u) \\ \vdots \end{bmatrix}$ can be put together to form a matrix $\boldsymbol{M}^{gb}$ (size *nq.nb*) so that all the corresponding Ψ^b vectors form the identity matrix, $\boldsymbol{I}_{nb \cdot \boldsymbol{nb}}$ (size *nb.nb*).

$$\boldsymbol{I}_{nb\cdot\boldsymbol{nb}} = \boldsymbol{M}^{bg} \cdot \boldsymbol{M}^{gb} \qquad \text{Eq. A8a}$$

$$(\boldsymbol{M}^{gb})^t = \boldsymbol{M}^{bg} \cdot (\boldsymbol{M}^{gb} \cdot (\boldsymbol{M}^{gb})^t) \qquad \text{Eq. A8b}$$

When $nb < nq$, $\boldsymbol{M}^{gb}$ is not invertible, so that the pseudoinverse approach is required. [27] In the present study, we multiply on the right by $(\boldsymbol{M}^{gb})^t$ (the transpose of $\boldsymbol{M}^{gb}$) to get Eq A8b. Then, the matrix $(\boldsymbol{M}^{gb} \cdot (\boldsymbol{M}^{gb})^t)$ on the right-hand-side of Eq. A8b is diagonalized and expressed as $(P^t \cdot D \cdot P)$. The pseudoinverse of $(\boldsymbol{M}^{gb} \cdot (\boldsymbol{M}^{gb})^t)$ is $\left(\tilde{P} \cdot \tilde{D}^{-1} \cdot \tilde{P}^t\right)$ where the tilde implies that only the non-zero eigenvalues, $\tilde{D}$, and their corresponding eigenvectors, $\tilde{P}$ are taken into account. In our case, the number of non-zero eigenvalues is the number of basis functions, *nb.* In that case, the matrix $\boldsymbol{M}^{bg}$, which is also the pseudoinverse of $\boldsymbol{M}^{gb}$, reads:

$$\boldsymbol{M}^{bg} = (\boldsymbol{M}^{gb})^t \cdot \left(\tilde{P} \cdot \tilde{D}^{-1} \cdot \tilde{P}^t\right) \qquad \text{Eq. A9}$$

For instance, in the present study, the basis set associated with the torsion is a Fourier series with 36 terms (cosine and sine functions) contracted with 24 basis functions. Furthermore, the number of grid points is 48 for both contracted and un-contracted basis sets. The largest difference (for k=1...nb and u=1...nq) between $\partial_x B_k(x_u)$ obtained from the usual relations of the orthogonal polynomials and the corresponding values obtained from the standard and the pseudoinverse approaches are given in table 3.

Table 3: Largest difference between $\partial_x B_k(x_u)$ obtained from the usual relations of the orthogonal polynomials and the corresponding values obtained from the standard (columns 2, 4) and the pseudoinverse (columns 3, 5) for the un-contracted (columns 2,3) and contracted (columns 4,5) basis sets.

largest error	*nb*=36 *nq*=48		*contracted, nb*=24 *nq*=48	
	Standard	Pseudoinverse	Standard	Pseudoinverse
$\partial_x B_k(x_u)$	$5.\ 10^{-14}$	$2.\ 10^{-14}$	$6.\ 10^{-5}$	$2.\ 10^{-14}$

The analysis of the results shows that when the Fourier basis set is not contracted the largest error on $\partial_x B_k(x_u)$ is of the same order of magnitude for the standard and the pseudoinverse procedure, while for the contracted basis set, the error obtained from the standard procedure is about 10^9 larger than the one obtained from the pseudoinverse approach.

Notes and references

[1] B. Podolsky, “Quantum-mechanically correct form of Hamiltonian function for conservative systems,” *Phys. Rev.*, vol. 32, no. 5, pp. 812–816, 1928.
[2] E. C. Kemble, *The Fundamental Principles of Quantum Mechanics*. New-York: Dover Publications, 2005.
[3] E. B. Wilson, J. C. Decius, and P. C. Cross, *Molecular vibrations : the theory of infrared and Raman vibrational spectra*, McGraw-Hil. New York, 1955.
[4] A. Nauts and X. Chapuisat, “Momentum, quasi-momentum and hamiltonian operators in terms of arbitrary curvilinear coordinates, with special emphasis on molecular hamiltonians,” *Mol. Phys.*, vol. 55, no. 6, pp. 1287–1318, Aug. 1985.
[5] F. Gatti, B. Lasorne, H.-D. Meyer, and A. Nauts, *Chpt. 6, Applications of Quantum Dynamics in Chemistry*, Springer International Publishing AG. 2017.
[6] X. Chapuisat and C. Iung, “Vector parametrization of the N-body problem in quantum mechanics: Polyspherical coordinates,” *Phys. Rev. A*, vol. 45, no. 9, pp. 6217–6235, 1992.
[7] F. Gatti, C. Muñoz, and C. Iung, “A general expression of the exact kinetic energy operator in polyspherical coordinates,” *J. Chem. Phys.*, vol. 114, no. 19, pp. 8275–8282, 2001.
[8] M. Ndong, L. Joubert-Doriol, H.-D. Meyer, A. Nauts, F. Gatti, and D. Lauvergnat, “Automatic computer procedure for generating exact and analytical kinetic energy operators based on the polyspherical approach.,” *J. Chem. Phys.*, vol. 136, no. 3, pp. 034107–034107, Jan. 2012.
[9] R. Meyer and H. H. Günthard, “General Internal Motion of Molecules, Classical and Quantum-Mechanical Hamiltonian*,” *J. Chem. Phys.*, vol. 49, no. 4, pp. 1510–1520, 1968.
[10] M. Harthcock and J. Laane, “Calculation of Kinetic Energy Terms for the Vibrational Hamiltonian: Application to Large-Amplitude Vibrations Using One-, Two-, and Three-Dimensional Models,” *J. Mol. Spectrosc.*, vol. 324, pp. 300–324, 1982.
[11] M. Senent, “Determination of the kinetic energy parameters of non-rigid molecules,” *Chem. Phys. Lett.*, vol. 296, no. November, pp. 299–306, 1998.
[12] D. Lauvergnat and A. Nauts, “Exact numerical computation of a kinetic energy operator in curvilinear coordinates,” *J. Chem. Phys.*, vol. 116, no. 19, pp. 8560–8560, 2002.
[13] E. Mátyus, G. Czakó, and A. G. Császár, “Toward black-box-type full- and reduced-dimensional variational (ro)vibrational computations,” *J. Chem. Phys.*, vol. 130, no. 13, p. 134112, 2009.
[14] D. Strobusch and C. Scheurer, “A general nuclear motion Hamiltonian and non-internal curvilinear coordinates.,” *J. Chem. Phys.*, vol. 138, no. 9, pp. 094107–094107, Mar. 2013.
[15] D. Lauvergnat and A. Nauts, “Quantum dynamics with sparse grids: a combination of Smolyak scheme and cubature. Application to methanol in full dimensionality,” *Spectrochim. Acta Part Mol. …*, vol. 119, pp. 18–25, Jun. 2014.
[16] J. Sarka, D. Lauvergnat, V. Brites, A. G. Császár, and C. Léonard, “Rovibrational energy levels of the F − (H 2 O) and F − (D 2 O) complexes,” *Phys Chem Chem Phys*, vol. 18, no. 26, pp. 17678–17690, 2016.
[17] W. Miller, N. Handy, and J. Adams, “Reaction path Hamiltonian for polyatomic molecules,” *J. Chem. Phys.*, vol. 72, pp. 99–99, 1980.
[18] T. J. Carrington and W. Miller, “Reaction surface Hamiltoian for the dynamics of reactions in polyatomic systems,” *J. Chem. Phys.*, vol. 81, no. November, pp. 3942–3950, 1984.
[19] C. Fábri, E. Mátyus, and A. G. Császár, “Numerically constructed internal-coordinate

Hamiltonian with Eckart embedding and its application for the inversion tunneling of ammonia," *Spectrochim. Acta - Part Mol. Biomol. Spectrosc.*, vol. 119, pp. 84–89, 2014.
[20] H. Tal-Ezer and R. Kosloff, "An accurate and efficient scheme for propagating the time dependent Schrödinger equation," *J. Chem. Phys.*, vol. 81, no. 9, pp. 3967–3967, 1984.
[21] D. Lauvergnat, S. Blasco, X. Chapuisat, and A. Nauts, "A simple and efficient evolution operator for time-dependent Hamiltonians: the Taylor expansion.," *J. Chem. Phys.*, vol. 126, no. 20, pp. 204103–204103, May 2007.
[22] E. R. Davidson, "The iterative calculation of a few of the lowest eigenvalues and corresponding eigenvectors of large real-symmetric matrices," *J. Comput. Phys.*, vol. 17, pp. 87–87, 1975.
[23] F. Ribeiro, C. Iung, and C. Leforestier, "A Jacobi-Wilson description coupled to a block-Davidson algorithm: an efficient scheme to calculate highly excited vibrational levels.," *J. Chem. Phys.*, vol. 123, no. 5, pp. 054106–054106, Aug. 2005.
[24] C. Lanczos, "An iteration method for the solution of the eigenvalue problem of linear differential and integral operators," *J. Res. Natl. Bur. Stand.*, vol. 45, no. 4, 1950.
[25] J. C. Light and T. Carrington Jr, "Discrete-variable representations and their utilization," *Adv. Chem. Phys.*, vol. 114, pp. 263–310, 2000.
[26] A. G. Császár, C. Fábri, T. Szidarovszky, E. Mátyus, T. Furtenbacher, and G. Czakó, "The fourth age of quantum chemistry: molecules in motion," *Phys. Chem. Chem. Phys.*, vol. 14, no. 3, pp. 1085–1085, 2012.
[27] R. Penrose and J. A. Todd, "A generalized inverse for matrices," *Math. Proc. Camb. Philos. Soc.*, vol. 51, no. 03, p. 406, Jul. 1955.
[28] J. Bowman, X. Huang, N. C. Handy, and S. Carter, "Vibrational Levels of Methanol Calculated by the Reaction Path Version of MULTIMODE , Using an ab initio, Full-Dimensional Potential," *J. Phys. Chem. A*, vol. 111, pp. 7317–7321, 2007.
[29] C. Muñoz-Caro, A. Niño, and M. L. Senent, "Theoretical study of the effect of torsional anharmonicity on the thermodynamic properties of methanol," *Chem. Phys. Lett.*, vol. 273, pp. 135–140, 1997.
[30] S. Blasco and D. Lauvergnat, "Quantum study of the internal rotation of methanol in full dimensionality (1+11D): a harmonic adiabatic approximation," *Chem. Phys. Lett.*, vol. 373, no. 3–4, pp. 344–349, May 2003.
[31] R. Dawes and T. Carrington, "How to choose one-dimensional basis functions so that a very efficient multidimensional basis may be extracted from a direct product of the one-dimensional functions: energy levels of coupled systems with as many as 16 coordinates.," *J. Chem. Phys.*, vol. 122, no. 13, pp. 134101–134101, Apr. 2005.
[32] G. Avila and T. Carrington, "Pruned bases that are compatible with iterative eigensolvers and general potentials: New results for CH 3 CN," *Chem. Phys.*, vol. 482, pp. 3–8, Jan. 2017.
[33] S. A. Smolyak, "Quadrature and Interpolation Formulas for Tensor Products of Certain Classes of Functions," *Sov. Math. Dokl.*, vol. 4, pp. 240–240, 1963.
[34] G. Avila and T. Carrington, "Nonproduct quadrature grids for solving the vibrational Schrödinger equation.," *J. Chem. Phys.*, vol. 131, no. 17, pp. 174103–174103, Nov. 2009.
[35] D. Lauvergnat and A. Nauts, "Torsional energy levels of nitric acid in reduced and full dimensionality with ElVibRot and Tnum.," *Phys. Chem. Chem. Phys.*, vol. 12, no. 29, pp. 8405–12, Aug. 2010.
[36] G. Avila and T. Carrington, "Using nonproduct quadrature grids to solve the vibrational Schrödinger equation in 12D.," *J. Chem. Phys.*, vol. 134, no. 5, pp. 054126–054126, Feb. 2011.
[37] J. Stare and G. Balint-Kurti, "Fourier Grid Hamiltonian Method for Solving the

Vibrational Schrödinger Equation in Internal Coordinates: Theory and Test Applications," *J. Phys. Chem. A*, vol. 107, pp. 7204–7214, 2003.
[38] Y. Scribano, D. Lauvergnat, and D. M. Benoit, "Fast vibrational configuration interaction using generalized curvilinear coordinates and self-consistent basis.," *J. Chem. Phys.*, vol. 133, no. 9, pp. 094103–094103, Sep. 2010.
[39] H. Wei and T. Carrington, "Discrete variable representations of complicated kinetic energy operators," *J. Chem. Phys.*, vol. 101, no. 2, pp. 1343–1360, Jul. 1994.